# REPORT DOCUMENTATION PAGE

Form Approved
OMB No. 0704-0188



| 1. AGENCY USE ONLY (Leave blank) | 2. REPORT DATE | 3. REPORT TYPE AND DATES COVERED |
|---|---|---|
| | 6/11/96 | STTR Phase I final report, 1Dec95 - 31May96 |

**4. TITLE AND SUBTITLE**

Small Efficient Thermophotovoltaic Power Supply
Using Infrared-Sensitive Gallium Antimonide Cells

**5. FUNDING NUMBERS**

DAAH04-96-C-0009

**6. AUTHOR(S)**

Dr. Lewis M. Fraas (PI on contract)

**7. PERFORMING ORGANIZATION NAME(S) AND ADDRESS(ES)**

JX Crystals Inc.
1105 12th Ave NW, Suite A2
Issaquah, WA 98027

**8. PERFORMING ORGANIZATION REPORT NUMBER**

**9. SPONSORING/MONITORING AGENCY NAME(S) AND ADDRESS(ES)**

U.S. Army Research Office
P.O. Box 12211
Research Triangle Park, NC 27709-2211

**10. SPONSORING/MONITORING AGENCY REPORT NUMBER**

ARO 35075.1-RT-STI

**11. SUPPLEMENTARY NOTES**

The views, opinions and/or findings contained in this report are those of the author(s) and should not be construed as an official Department of the Army position, policy, or decision, unless so designated by other documentation.

**12a. DISTRIBUTION/AVAILABILITY STATEMENT**

Distribution authorized to U.S. Government Agencies only; report contains proprietary data produced under STIR contract. Other requests shall be referred to the performing organization in Block 7 of this form.

**12b. DISTRIBUTION CODE**

**13. ABSTRACT** *(Maximum 200 words)*

Under Phase I, JX Crystals has increased the power output from its cylindrical thermophotovoltaic generator from 71 Watts to 132 Watts and it has developed a better understanding of the thermal design parameters. Independently, it has discovered an infrared emitter with a spectral output which is very well matched to the spectral response for its GaSb cells. Using this new emitter, JX Crystals predicts that the output of its thermophotovoltaic generator can still be substantially improved.





| 14. SUBJECT TERMS | 15. NUMBER OF PAGES |
|---|---|
| thermophotovoltaic, gallium antimonide, GaSb, infrared, IR | 16 |
| | 16. PRICE CODE |

| 17. SECURITY CLASSIFICATION OF REPORT | 18. SECURITY CLASSIFICATION OF THIS PAGE | 19. SECURITY CLASSIFICATION OF ABSTRACT | 20. LIMITATION OF ABSTRACT |
|---|---|---|---|
| UNCLASSIFIED | UNCLASSIFIED | UNCLASSIFIED | UL |

# JX Crystals Inc. - Army STTR Phase I Final Report 6/7/96

Proposal Title: Small Efficient Thermophotovoltaic Power Supply Using Infrared-Sensitive Gallium Antimonide Cells

Contract # : DAAH04-96-C-0009

## Phase I Objectives

The idea of producing electricity by surrounding a man-made heat source with photovoltaic cells has many attractive features. The fact that these thermophotovoltaic generators will run silently is perhaps the most important feature for the army followed by the fact that these generators should be intrinsically lightweight.

The first challenge in reducing the above idea to practice is to pick the appropriate photovoltaic cell. Initially, the silicon photovoltaic cell was picked because of its immediate availability. However, time has shown that the required emitter temperatures of over 2000° C are unattainable in stable operation and that even when these emitter temperatures are attained for short time periods, the resultant chemical to radiation conversion efficiencies are very small.

While some early workers recognized these problems with silicon and turned to germanium, there were problems with germanium cells. Experimentally, germanium cell voltages were very low because of problems with germanium oxide and, theoretically, germanium cell current densities are limited to low values via the Auger recombination limit imposed on indirect gap materials.

A viable low bandgap photovoltaic cell for use with man-made heat sources first became available in 1989 with the demonstration of the GaSb cell by a team then at Boeing led by the present author. This cell responds out to 1.8 microns which is near ideal for an emitter temperature of 1500° C. A positive feature inherent in this cell is its direct bandgap which allows very high current densities and, hence, power densities to be attained. Additional positive features relate to manufacturing cost. The cell process copies silicon cell processing in that diffusions are used for junction formation and low pressure converted silicon crystal pullers are used for GaSb crystal growth.

More recently, GaInAs/InP low bandgap cells have become available. Although these direct gap cells have performances similar to those of the GaSb cell, the process used in fabricating these cells uses epitaxy with toxic gases for the InGaAs layer growth and high pressure pullers for InP crystal growth. These processes are intrinsically much more expensive and more dangerous than the processes used to fabricate GaSb cells.

For the above reasons, we proposed on this Phase I contract developing a TPV electric generator by surrounding a flame heated infrared emitter with GaSb photovoltaic cells. Our primary objective for this work was to demonstrate a fuel fired thermophotovoltaic generator that produced over 100 W of electric power. We accomplished this objective. In order to accomplish this objective, we fabricated GaSb TPV cells, filters, circuits, and a complete receiver assembly for this fuel fired TPV generator and we fabricated an improved spine-disc emitter / burner and demonstrated its high temperature operation. Having built this first test bed unit, we have been able to begin developing a more optimum IR emitter and to begin to develop a comprehensive thermal model for this TPV generator.

## TPV Generator Design Review

Having picked the most appropriate TPV cell, the GaSb cell, and a target emitter temperature, 1500° C, the next most important challenge is to design an IR emitter configuration which maximizes the TPV system's radiation to electric conversion efficiency. Figure 1 shows the "IR selective" emitter configuration we chose to work with during our phase I effort. In this configuration, the combination of a SiC blackbody emitter, quartz heat shields, and a dielectric filter serves as a selective emitter. While the SiC blackbody emits at all wavelengths, the quartz heat shields return the energy in wavelengths longer than 3.5 microns back to the emitter and the dielectric filter returns the energy in the wavelength band between 1.8 and 3.5 microns back to the emitter. The result is that only the radiation with wavelengths less than 1.8 microns is transmitted to the cells while the remaining energy is recycled to the emitter.

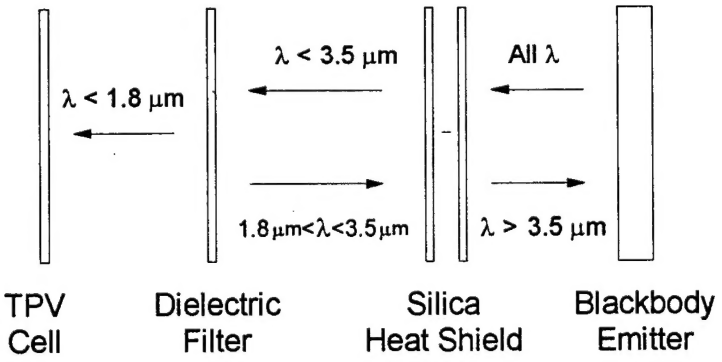


Fig 1: Emitter concept

Figure 2 shows the results of the calculation for this multi-component emitter concept. This is the concept we implemented during our phase I activity. As we will discuss later, there are problems with this concept for small TPV generators. However, we will describe an improved matched emitter.

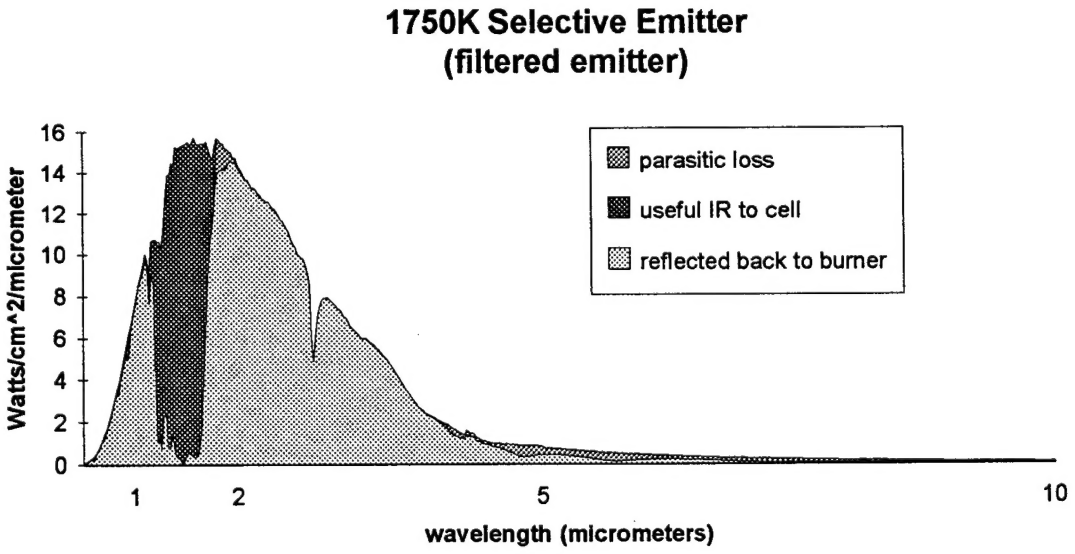


Fig 2: Graphic projected emitter performance

An electric generator has to be designed to convert chemical energy into electrical energy efficiently. For a TPV generator, this problem can be divided into two problems: first, the conversion of chemical energy into radiation energy and second, the conversion of radiation energy into electric energy. So far, the discussion of cells and emitters has dealt with the second half of the problem, the radiation to electric conversion problem. Figures 3 and 4 here describe how we handle the chemical to radiation conversion problem. Figure 3 shows schematically the complete TPV generator design and figure 4 shows the burner / emitter design in more detail.

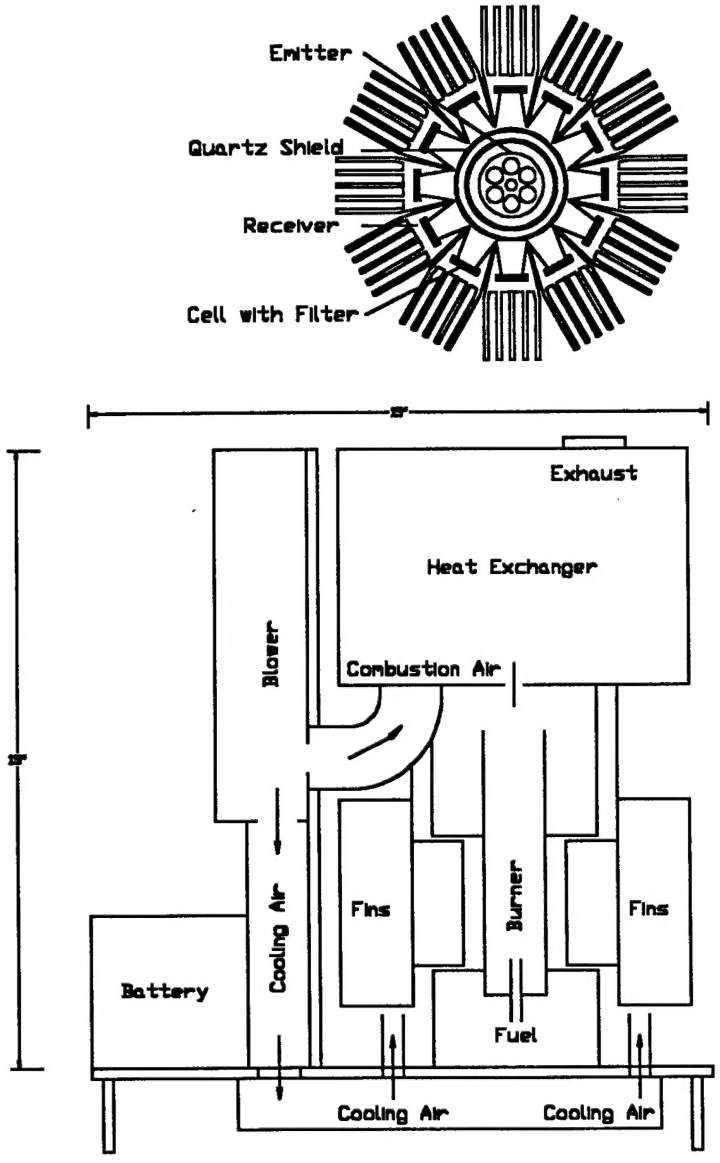


Fig 3: 100 W air-cooled TPV generator design

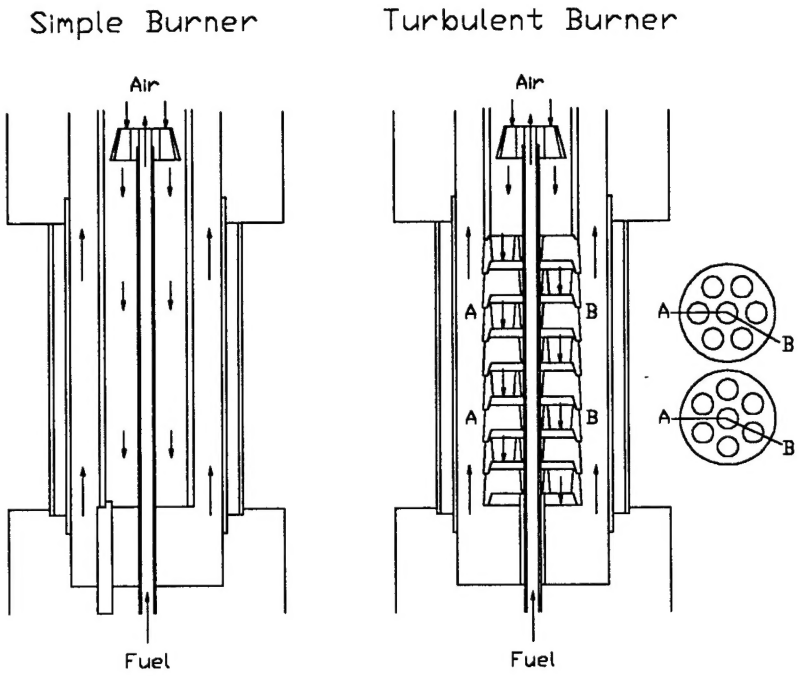


Fig 4: Burner / emitter design

Referring to figure 4, fuel and air are mixed and burned in a section just above the emitter. In the simplest design, the emitter is just an open-ended SiC tube which is heated by an inside down-pass and again by an outside up-pass of the hot combustion gases. The problem with this design is that the gas heat transfer efficiency is poor. The solution to this problem is to create turbulence in the gases by using spine-discs to fabricate the emitter as shown on the right in figure 4. This spine-disc concept also allows for adjustments in the emitter temperature profile from top to bottom by adjusting the relative rotations of the discs in the column.

Returning to a discussion of chemical to radiation efficiency, if the combustion air supplied at the top of the burner were to be supplied at room temperature, the gas temperature immediately after combustion at the top inside of the emitter would then be the adiabatic flame temperature of 2100° C. Then given sufficient turbulence and heat transfer through the emitter and given an emitter temperature of 1500° C, the gas temperature at the top outside of the emitter would have dropped to 1500° C. This drop in gas temperature of 600° C means that the chemical to radiation conversion efficiency is only 600/2100 = 29%. This conversion efficiency can be dramatically increased by using a counterflow heat exchanger to extract energy from the exhaust gases and preheat the combustion air. For example, if the preheated combustion air allows a flame temperature of 2600° C while exhaust gases are cooled to 700° C, extracting 1900° C from the gases means that the chemical to radiation efficiency can be increased to 1900/2600 = 73%. For this reason, our TPV test unit design incorporates a heat exchanger as shown in figure 3.

## Accomplishments

We began this project by fabricating 200 GaSb cells in two lots. The first lot consisted of 160 cells with illuminated areas of 1.25 $cm^2$ and the second lot consisted of 40 cells with illuminated areas of 1.75 $cm^2$. The larger area cells were designed to be located at the ends of each circuit in order to accommodate emitter intensity fall off at each end.

All cells were qualified by flash testing. Then a typical cell from the first lot was soldered to a water cooled assembly and tested in front of a SiC blackbody emitter operating at 1380° C (1650 K). Figure 5 shows the illuminated current vs. voltage curve from this test. The cell produced a current of 5.9 Amps for a current density of 4.7 $A/cm^2$ and a power of 1.75 W for a power density of 1.4 $W/cm^2$. These values are close to the predicted values indicating that the cell performance is within range.

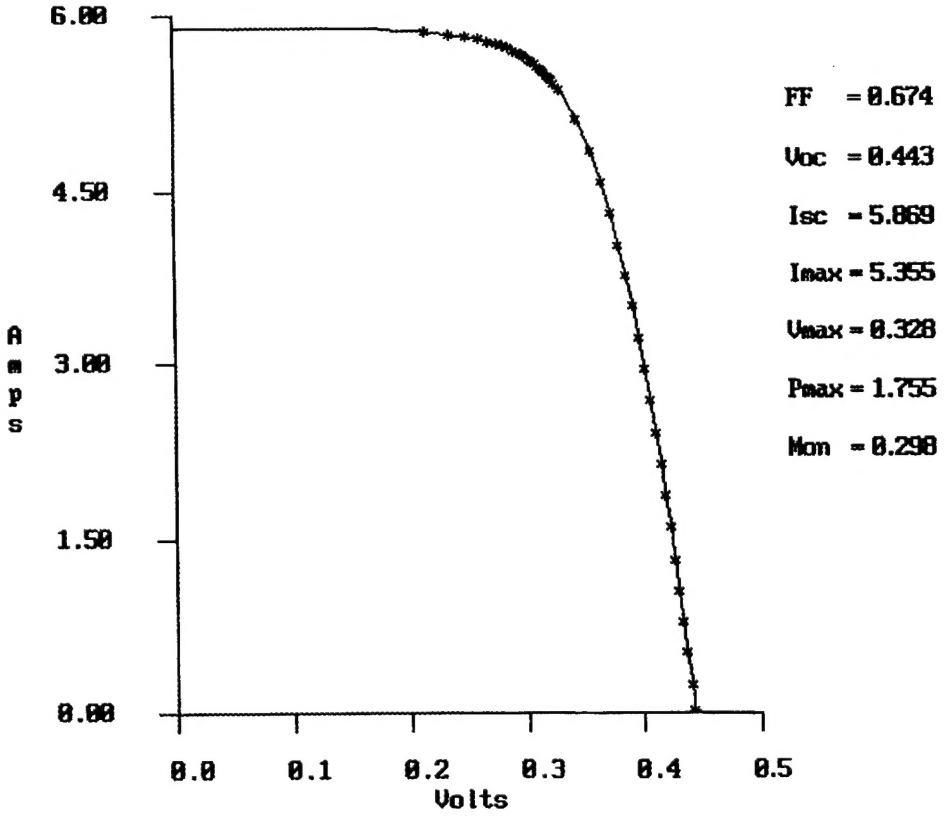


Fig 5: Illuminated current vs. voltage curve for water cooled GaSb cell tested in front of SiC emitter with 1380° C emitter temperature.

Next, we designed and fabricated 12 circuits with each circuit containing 12 smaller cells and 2 large end cells all wired in series. The circuit design targeted a voltage output of over 4 V per circuit. We adjusted the distance from the flash lamp to produce approximately 4 A per circuit and tested all 12 circuits. The test results are shown in table 1. All 12 circuits performed well.

Table 1: Circuit performance

| circuit | FF | Voc | Isc | Imax | Vmax | Pmax | Light Level |
|---|---|---|---|---|---|---|---|
| 1 | 0.723 | 6.885 | 4.037 | 3.647 | 5.508 | 20.086 | 0.085 |
| 2 | 0.747 | 6.958 | 4.191 | 3.832 | 5.684 | 21.782 | 0.085 |
| 3 | 0.729 | 6.901 | 4.195 | 3.708 | 5.693 | 21.11 | 0.084 |
| 4 | 0.723 | 6.902 | 4.013 | 3.619 | 5.532 | 20.023 | 0.084 |
| 5 | 0.703 | 6.836 | 3.972 | 3.462 | 5.513 | 19.085 | 0.086 |
| 6 | 0.745 | 6.855 | 4.166 | 3.844 | 5.537 | 21.283 | 0.087 |
| 7 | 0.731 | 6.881 | 4.176 | 3.826 | 5.493 | 21.017 | 0.086 |
| 8 | 0.735 | 6.88 | 4.063 | 3.618 | 5.679 | 20.545 | 0.086 |
| 9 | 0.731 | 6.902 | 4.058 | 3.696 | 5.537 | 20.464 | 0.086 |
| 10 | 0.74 | 6.898 | 3.94 | 3.611 | 5.571 | 20.116 | 0.087 |
| 11 | 0.715 | 6.864 | 4.101 | 3.568 | 5.645 | 20.139 | 0.086 |
| 12 | 0.716 | 6.83 | 3.99 | 3.576 | 5.459 | 19.523 | 0.086 |

We then fabricated IR filters and mirrors and bonded the filters and mirrors to the circuits and the circuits to heat sinks. We then fabricated the cylindrical receiver assembly shown in figure 6. This cylinder contained two half cylinder groups of circuits wired in parallel with each group generating over 24 V. Each half cylinder group contained 6 circuits wired in series.

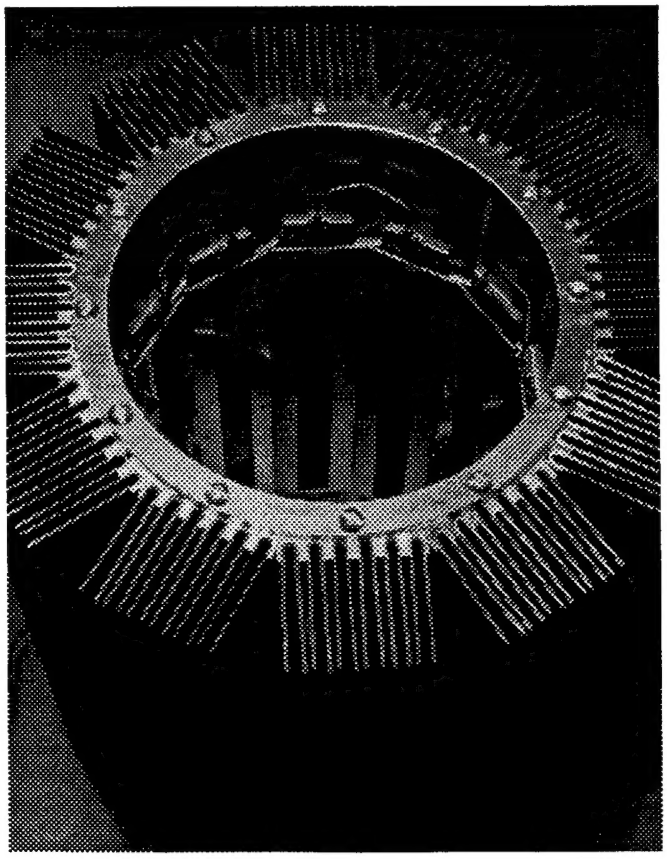

Fig 6: Photo of new receiver cylinder

Turning to the construction of the SiC emitter spine discs, we obtained 11 high quality SiC spine discs from Dow Corning and 16 SiC spine discs from Western Washington University. Our thermal testing has shown that the Dow Corning spine discs operate without degradation at 1600° C whereas the mortar in the WWU discs softened at approximately 1350° C. Figure 7 shows a photo of the Dow Corning SiC spine discs.

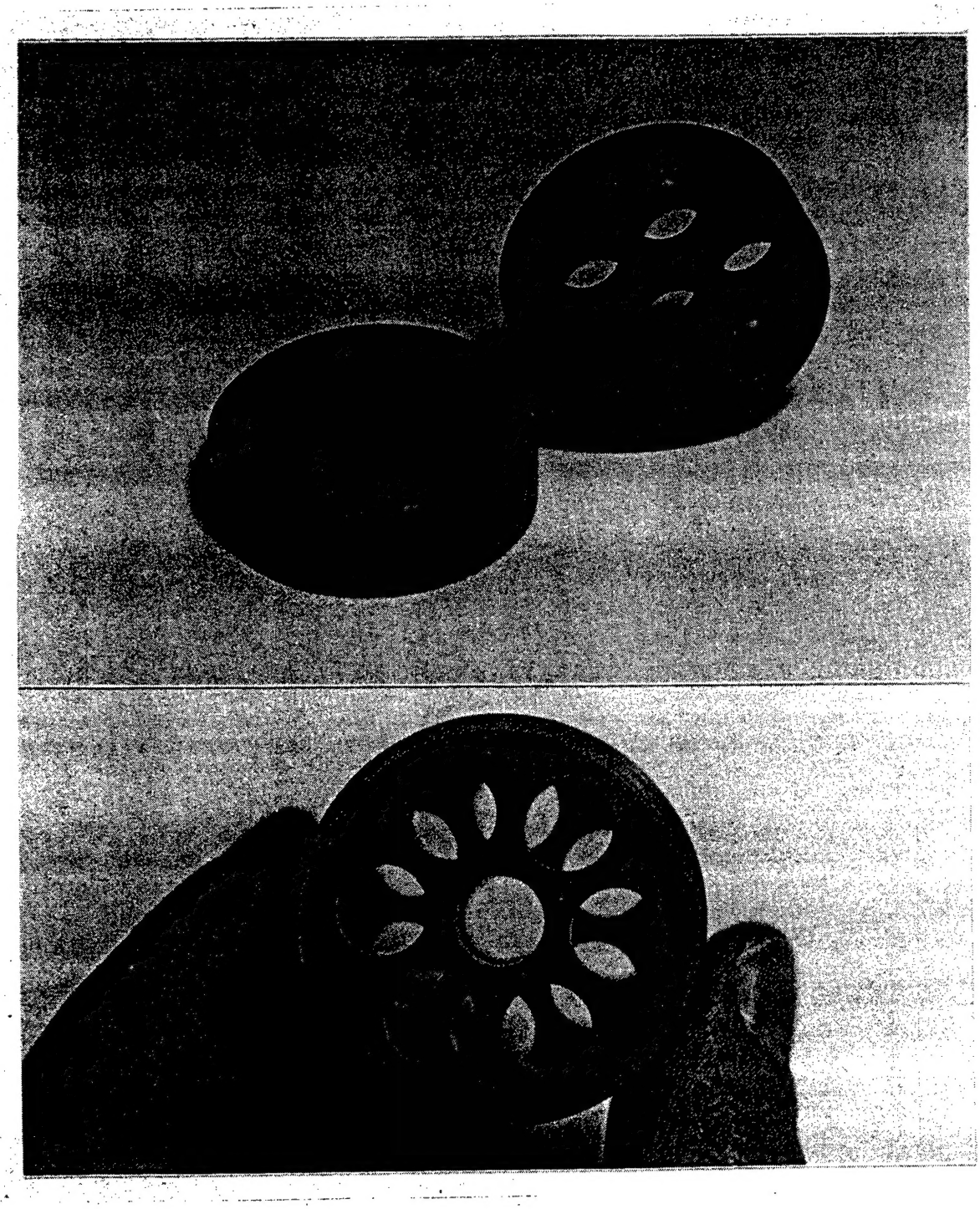

Fig 7: Photo of Dow Corning SiC spine discs

We had previously built a heat exchanger and support structures which we combined with the new parts to fabricate our TPV test unit. Figure 8 shows a photograph of this unit in operation.

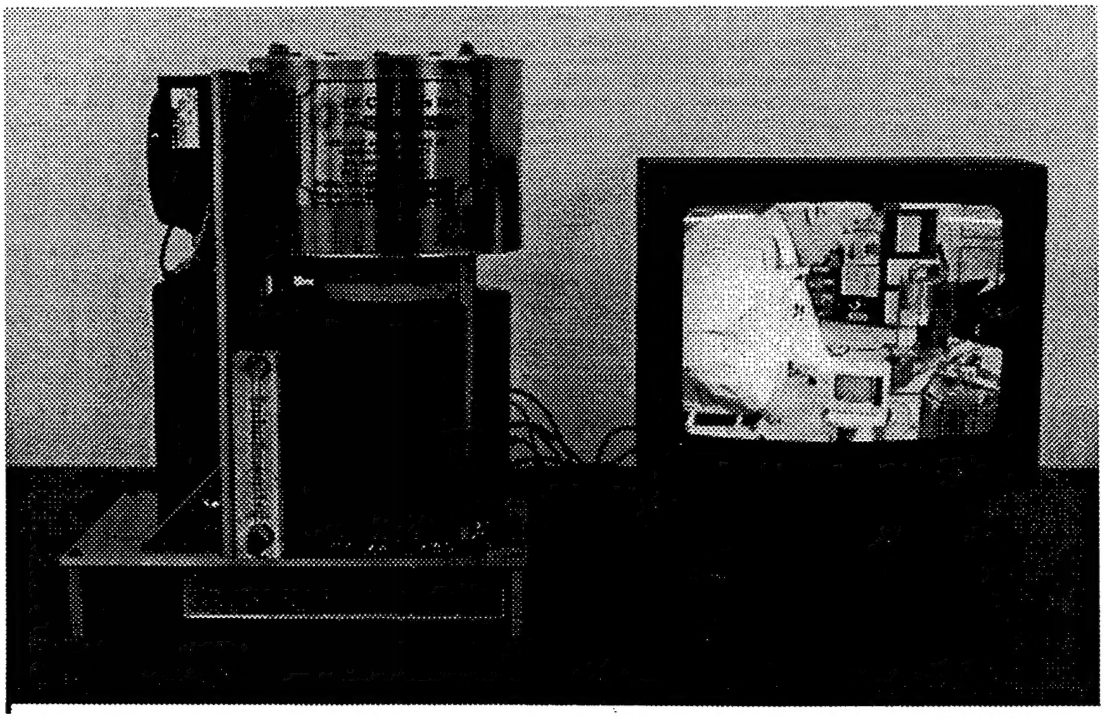

Fig 8: Photo of operating generator

Table 2 summarizes our test results for our TPV cylindrical generator. An explanation of these results line by line follows. We had begun work on this cylindrical generator using IR & D funds prior to the start of this contract in December of 1995. This work used the simple tubular emitter and a 12 V cylindrical receiver assembly containing twelve 7 cell circuits . We had also obtained the Dow Corning spine discs. Using this spine disc emitter along with an improved combustion air blower supplying more combustion air thence allowing more fuel, we improved the current output of our generator to 6 Amps at the start of this project in December. This corresponds to 3 Amps per circuit.

By March of 1996, we had completed the fabrication of the 24 V cylinder shown in figure 6 and we had received new spine discs from Western Washington University. However, our first test with this new combination was disappointing. We only obtained 3 Amps when we had hoped for over 6 Amps.

Our analysis shown in more detail in the next section indicates that the emitter was not running hot enough. Our explanation for this is as follows: The emitter concept described in figure 1 with energy being returned to the emitter was predicated on an assumption of infinite parallel planes of cell, filter, and emitter. While this assumption will be more valid for larger generators, it is not true for our current generator. The emitter diameter in our current generator is only 1.5 " whereas the cells

are located on the inside surface of a 4.5" diameter cylinder. Furthermore, the emitter for the 7 cell circuit case is only 3.5" long. First, it is obvious that there are major end loses. It is probably also true that circulating non-radial modes develop for radiation paths where the radiation does not return to the emitter. The result is that the radiation recycling efficiency is only a fraction of what was initially assumed.

Table 2: JX Crystals' "Midnight Sun®" Air Cooled TPV Generator History

| Date | Comment | Voltage | Current |
|---|---|---|---|
| March 1995 | 1st completely functional unit | 12 V | 2 Amp |
| July 1995 | Improved cooling | 12 V | 4 Amp |
| *Dec 1995 | *Spin-Disc Emitter | *12 V | *6 Amp |
| *March 1996 | *Larger circuits | *24 V | *3 Amp |
| *April 1996 | *Improved emitter | *12 V | *11.4 Amp |

*Army STTR

Given the above arguments, we reasoned that we needed a more selective emitter than SiC operating at a higher temperature. Separate emitter experiments on smaller Bunsen burner units had taught us that platinum was a somewhat selective emitter and that platinum had a lower emissivity in the cell response band. We had been experimenting with platinum glazings on ceramics as a low cost way of using a platinum emitter. We therefore glazed the outer surfaces of the Dow Corning spine discs and returned to the 7 cell circuits because we did not have enough high temperature survivable discs for the new 24 V cylinder. The final line in table 2 confirmed that our reasoning was correct. We obtained over 11 Amps with the improved emitter discs. The generator power output went to 130 W, a new high for us.

However, our final conclusion is that we still need to work on improving infrared emitters for use with our cells in TPV systems. We also need to improve our theoretical understanding of the thermal system. In the next section, we sketch a simple model for understanding the results we have recently observed. This model can serve as a framework for a more complete model yet to be developed.

**Theoretical Model**

The energy flow diagram for our TPV system is shown in figure 9. Chemical energy is introduced into the combustion section where energy is either coupled to the emitter or enters the heat exchanger. From the emitter, there is an energy flow path to the cell receiver by both radiation and conduction/convection. There are two energy recuperation paths. The radiation recycling path is shown vertically in figure 9. There is also an exhaust recuperation path through the heat exchanger. In the end, the energy leaves the system as electric power or as heat. The waste heat leaves either by heat removed from the cell receiver fins or by heat leaving with the exhaust gases or through heat escaping from the housing structures.

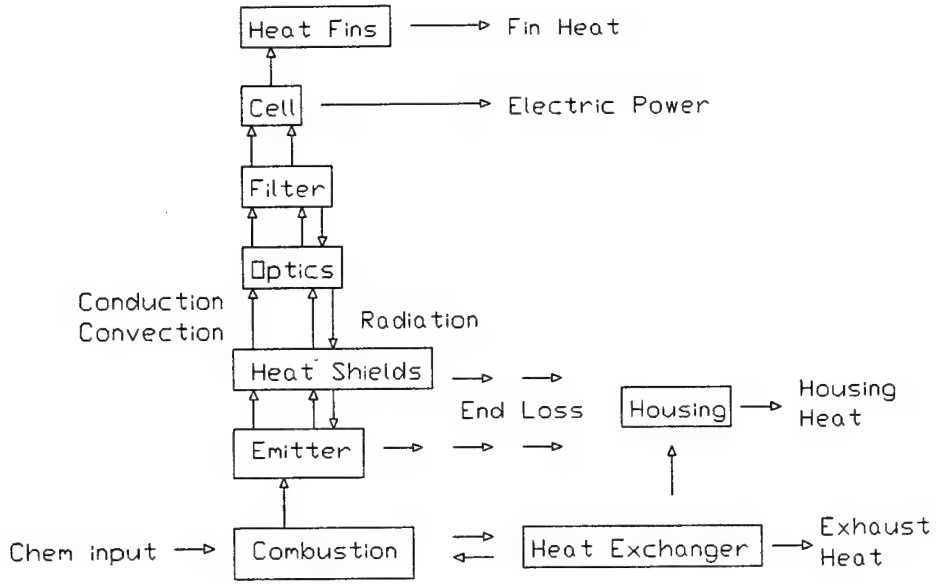


Fig 9: General Theory

In the following discussion, we focus on a calculation of the two cell receiver performance parameters which we define as the electric power out and the ratio of electric power out to receiver heat load. We define the ratio of electric power out to receiver heat load as the receiver efficiency with the additional note that the receiver heat load is measured when the receiver is delivering its maximum electric power. It must be remembered that the receiver will have to handle the higher heat load at open circuit.

During our phase I effort, we used a counterflow heat exchanger but we made no effort to measure or quantify its performance. So, we do not attempt to model it here. Herein, we focus on the energy flow path from the emitter. In our TPV cylinder design, we use multiple concentric cylindrical quartz heat shields surrounding the emitter. These heat shields serve two functions. They are both radiation shields and they serve to eliminate convection currents. If in fact convection currents have been eliminated, then the conduction and convection heat transfer paths should be small compared to the radiation heat transfer paths. This will need to be verified by future measurement. In the following discussion, we focus on the radiation heat transfer model.

Our first goal was to calculate the cell current and hence cell electric power given an emitter model. For our phase I activity, we used a SiC emitter which can be modeled as a graybody. We begin, therefore, with a model of a blackbody. Table 3 summarizes the appropriate blackbody equations for calculating cell current. The most significant point is that there is an accurate closed form approximation for the cell current that is valid for an emitter temperature range between 900° C and 1500° C for a GaSb cell with a band edge at 1.8 microns. As table 3 shows, this approximation is based on dropping the 1 in the denominator in the blackbody integral, an approximation which is valid at shorter wavelengths. The solid and dashed curves in figure 10 show that this assumption is valid for GaSb cells over the useful system temperature range just stated.

## Table 3: Blackbody theory for TPV

### Definitions:

$\theta = \frac{T}{T_o}$; T= emitter temp.; $T_o$ = room temp.

$$x = \frac{h\nu}{kT}; x_o = \frac{h\nu_o}{kT} = \frac{E_g}{kT}$$

where $E_g$= cell bandgap energy

### Blackbody Flux

$$I = \sigma T^4 = \frac{15}{\pi^4}\sigma T^4 \int_0^\infty B(x)\,dx$$

where $B(x) = \frac{x^3}{e^x - 1} \cong x^3 e^{-x}$

### Photon Flux

$$n_\phi = \frac{15}{\pi^4}\sigma T_o^4 \theta^4 \int_{x_o}^\infty \frac{1}{h\nu}\frac{x^3}{e^x - 1}dx = \frac{\sigma T_o^3}{k}\theta^3\phi$$

$$\phi \cong \frac{15}{\pi^4}\int_{x_o}^\infty x^2 e^{-x}dx = \frac{15}{\pi^4}(x_o^2 + 2x_o + 2)e^{-x_o}$$

$j = n_\phi q = j_o \theta^3 \phi$ where $j_o = 1.57\,A/cm^2$

for $\lambda_o$=1.8 μm, $\phi \cong 0.025(\theta - 4)$

$\theta$=6 $\Rightarrow$ T=1800 K = 1500 C

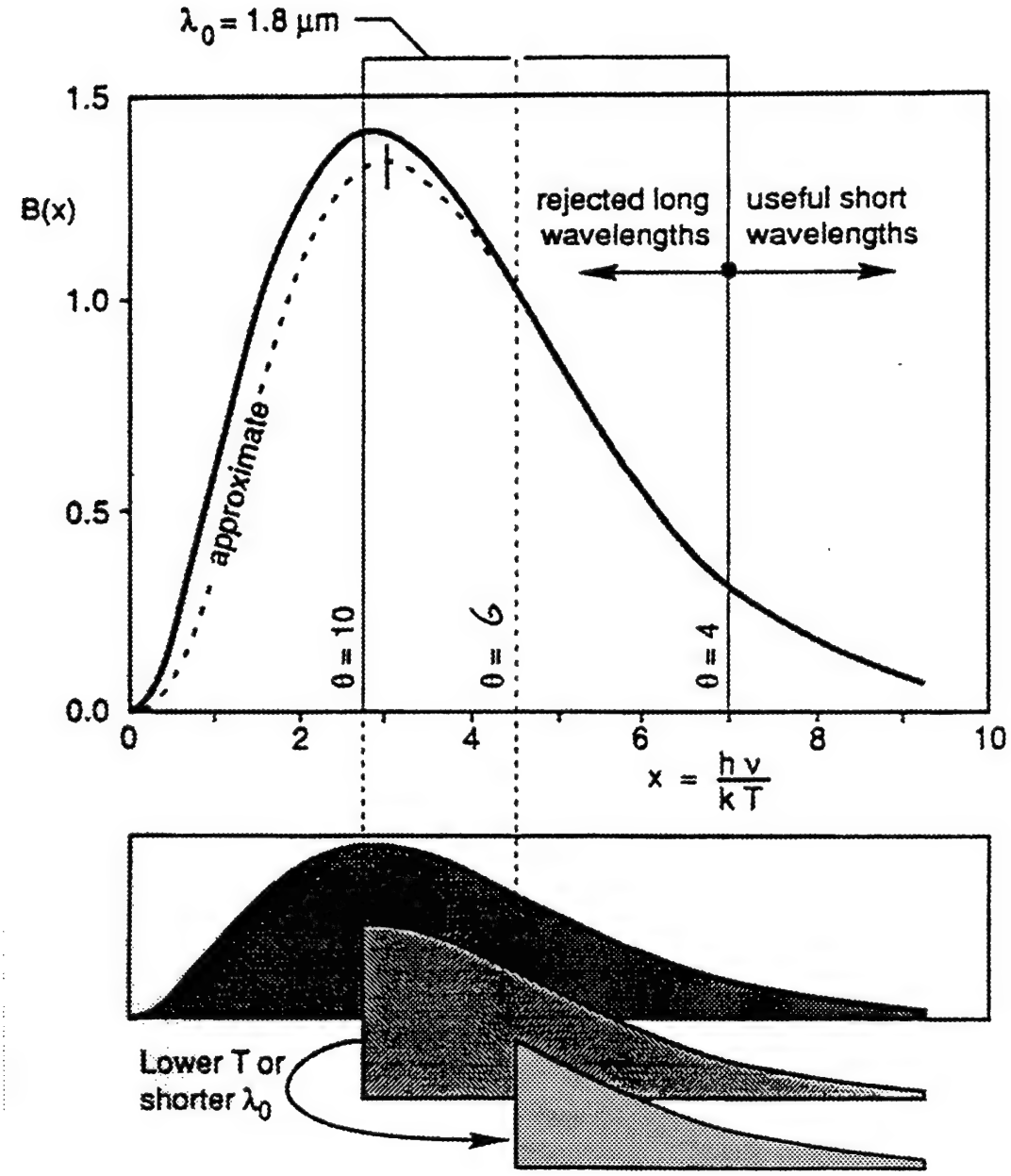


Fig 10: Graphs of exact and approximate blackbody functions

In our phase I proposal, we dealt with the radiation transfer problem by first stating an emitter temperature and then calculating the cell current. However, during our phase I experimental work, we found it more practical to define the amount of heat we could dissipate in the cell receiver and then to calculate the emitter temperature and then the cell current. Table 4 summarizes the procedure we have adopted. In this table, we first list the appropriate equations for forced air cooling. Then we list the calculation procedures, and finally we give a specific example. The example given is close to our phase I calculated performance goal.

Table 4: New calculation procedure

**Theory - Forced Air Cooling:**

$Q = (5/2)\ R\ \Delta T\ F$
$F$ = 80 cu ft / min = 36 liter / sec
$\Delta T$ = 40 C
$R$ = 8.3 joule / mole K
**$Q$ = 1,330 Watts**

**Theory - Receiver Efficiency Calculation Procedure:**

1) State chemical input power, radiation recycling efficiency, and emissivity.
2) Calculate radiated power.
3) Calculate emitter temperature.
4) State cell view factor and average quantum yield.
5) Calculate cell current.
6) State cell maximum power voltage and calculate cell power.
7) Calculate receiver electrical efficiency.

**Theory - Calculation Procedure - Example:**

1) Chemical input power = 1310 W; Emitter Area = 100 $cm^2$;
   Radiation Recycling Efficiency = 70%; Emissivity = 0.8.
2) Radiated Power = 13.1 / 0.3 = 43.7 W / $cm^2$
3) $T^4 = 43.7 / (\sigma\varepsilon)$
   T = 1760 K = 1490 C; $\theta$=5.9; $\phi$=.048.
4) Cell View Factor = 0.75; Average Quantum Yield = 0.75.
5) Cell Current = $j = j_o\ \theta^3\ \phi\ \varepsilon$ vf QE = 6.96 Amp / cm2.
6) Cell Maximum Power Voltage = 0.33 V; Cell Array Power = 232 W.
7) **Receiver Electrical Efficiency = 232 / (1310-232) = 22%.**

The key difference between our proposal procedure and this new procedure is that we have introduced a radiation recycling efficiency parameter in the new procedure. When this parameter is near 70%, we are modeling the infinite parallel plane case initially assumed. However, a lower recycling efficiency allows for end losses and scattering of radiation into circulating non-radial modes in the cylindrical geometry.

It is now possible to adjust the radiation recycling efficiency parameter to fit various phase I measured results and to make a prediction for phase II. Case 1 in table 5 is the case calculated in table 4 assuming 70% recycling. However, case 2 is the situation we actually observed in Dec of 1995 where the radiation recycling parameter has been reduced to 40%. Case 3 is the case we predicted and observed for the platinum glazed spine discs at the end of the phase I effort. Reducing the emitter emissivity from 0.8 for SiC to 0.3 for platinum makes the emitter run hotter which shifts more radiation to shorter wavelengths producing more current.

Table 5: Explanation for Phase I results and prediction for Phase II

| | P(in) | Recycling | Emissivity | T(°C) | P(out) | Efficiency |
|---|---|---|---|---|---|---|
| Case 1: | 1310 W | 0.7 | 0.8 | 1490 | 232 W | 22 % |
| Case 2: | 1310 W | 0.4 | 0.8 | 1210 | 71 W | 6 % |
| Case 3: | 1310 W | 0.4 | 0.3 | 1620 | 132 W | 11 % |
| Case 4: | 1310 W | 0.4 | matched | 1490 | 225 W | 21 % |

However, the primary lesson learned is that for small geometries, the radiation recycling efficiency is not as high as we would have liked and it is therefore preferable to find a more matched emitter which does not radiate as much non-useful radiation in the first place. Case 4 in table 5 is a prediction of performance for such a matched emitter. The next section presents preliminary data on this new matched emitter. We plan to develop a TPV generator using this new emitter in our phase II effort.

**IR & D Matched Emitter**

Fortunately on a separate IR & D project, we had been working on a Bunsen burner demonstration unit which used a 0.75" diameter, 1" tall emitter. This emitter was so small that it was obvious that it would be difficult to return radiation to it. We therefore had looked for, and fortunately, had found a very promising emitter.

In April of 1996, JX Crystals discovered an infrared emitter which is nearly perfectly matched to our GaSb infrared cell. Figure 11 shows one of these glowing emitters and figure 12a shows the emittance for this new material. As figure 12a shows, this new material emits strongly for wavelengths where our cell responds and weakly for longer wavelengths where our cell does not respond. Unlike previous rare earth oxide selective emitters, the bandwidth of this new emitter corresponds nearly perfectly with the cell bandwidth rather than being much narrower. The narrow bandwidths associated with rare earth oxide selective emitters severely restrict available power densities.

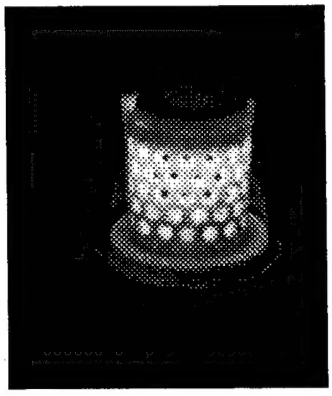

Fig 11: Photo of matched emitter

Figure 12b shows the advantage of this new emitter relative to a blackbody. For the same chemical input energy, this emitter will run hotter than a blackbody emitter and the power available to our cell from this new emitter is increased by a factor of four. This new emitter promises to make Midnight Sun® generators more powerful and more efficient. The next step is to make spine discs from this new matched emitter material.

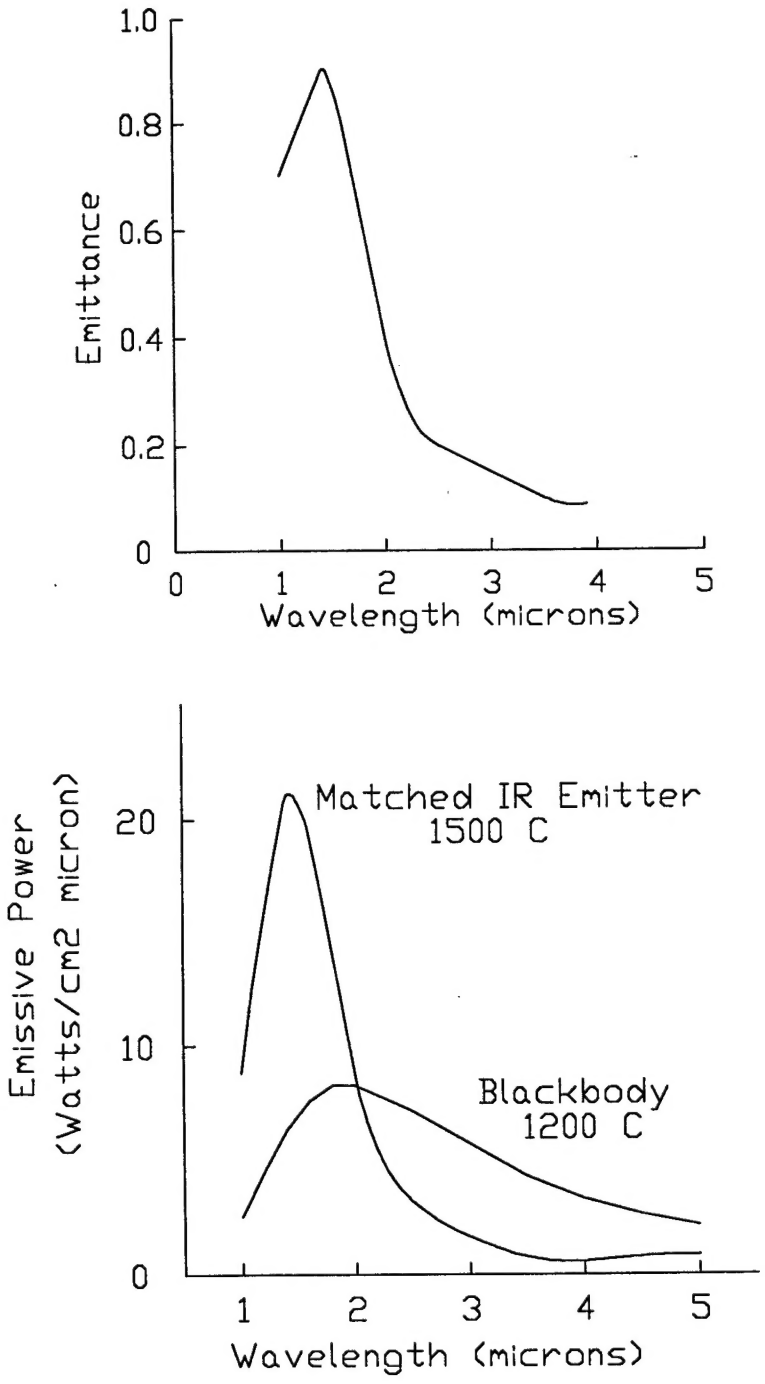


Fig 12a & b: Emittance and emissive power for matched emitter

## Conclusions

Over the time period of our phase I effort, we have increased the power output from our cylindrical TPV generator from 71 Watts to 132 Watts and we have developed a better understanding of the thermal design parameters. We have also independently discovered an infrared emitter with a spectral output which is very well matched to the spectral response of our GaSb cells. Using this new emitter, we predict that the output of our TPV generator can still be substantially improved.